

INFLUENCE OF PARTICLE INTERACTION ON THE FORM OF THE BRAGG CURVE

I. M. VASILEVSKIĬ, I. I. KARPOV, and Yu. D. PROKOSHKIN

Joint Institute for Nuclear Research

Submitted July 24, 1968

Zh. Eksp. Teor. Fiz. 55, 2166-2172 (December, 1968)

A comparison is made of the form of the measured and calculated Bragg curve, for protons, deuterons, and  $\alpha$  particles with momentum  $\approx 1.3$  GeV/c. It is shown that the form of the Bragg curve depends strongly on the geometry of the experiment and that in the calculation of the Bragg curve for high-energy particles it is necessary to take into account the nuclear interaction of these particles with the stopping substance.

I. INTRODUCTION

THE range  $R_0$  of heavy charged particles in a substance is connected with the particle energy  $E_0$  by the relation

$$R_0 = \int_0^{E_0} \left( \frac{dE}{dR} \right)^{-1} dE, \tag{1}$$

which makes it possible to determine the value of  $E_0$  by measuring  $R_0$ . The ionization energy loss  $dE/dR$  which enters in (1) is described by the Bethe-Bloch formula

$$-\frac{dE}{dR} = \frac{2\pi(Ze^2)^2n}{\rho mc^2\beta^2} \left\{ \ln \frac{2mc^2\beta^2T}{I^2(1-\beta^2)} - 2\beta^2 - \frac{2}{Z} \sum_{K,L,\dots} C_i - \delta \right\}, \tag{2}$$

where  $\beta$  is the velocity of the particle in units of the velocity of light  $c$ ,  $Ze$  is its charge,  $m$  is the electron mass,  $n$  is the number of electrons per  $\text{cm}^3$  of the substance,  $\rho$  is the density of the substance,  $T$  is the maximum energy transferred to the electron,  $I$  is the average ionization potential of the atoms of the substance,  $C_i$  are corrections which take into account the coupling of the electrons on the  $K, L, \dots$  shells of the atom<sup>[1]</sup>, and  $\delta$  is a correction for the density effect<sup>[2]</sup>. In the case when the particle energy  $E$  is large (hundreds of MeV), the corrections  $C_i$  are small and can be accurately calculated<sup>[1]</sup>, while the ionization potential  $I$  is determined experimentally accurate to 2-3%<sup>[2]</sup>. This corresponds to an uncertainty not exceeding  $(2-4) \times 10^{-3}$  in the calculation of the "range-energy" relation ( $dE/dR$ ) depends logarithmically on  $I$ .

One of the widely used methods of determining the range  $R_0$  is to measure the Bragg curve  $B(R)$ , namely the dependence of the current  $B$  of the ionization chamber that detects the particles after passing through a layer of the substance on the thickness of this layer  $R$ . In the idealized case, when it is possible to disregard straggling, the initial spread of the particles with respect to the energy  $E$ , and the scattering of the particles in the stopping substance, we have  $B(R) \sim dE/dR$  (Fig. 1). Allowance for straggling and for the particle-energy spread changes the form of the Bragg curve in the region  $R \approx R_0$  (Fig. 1).

Measurements of the ranges of high-energy protons<sup>[3-5]</sup> have shown that the experimentally determined Bragg curve  $R \gtrsim R_0$  agrees with the  $B(R)$  dependence calculated with allowance for the fluctuations

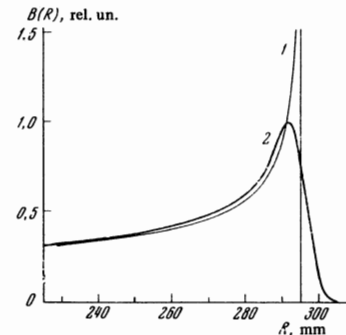


FIG. 1. Calculated Bragg curves for protons with range  $R_0 = 295$  mm for copper: 1—idealized ( $dE/dR$ ) curve calculated without allowance for the straggling, the spread of the energy of the beam proton, and the interaction of the protons with the substance; 2—Bragg curve calculated with allowance for straggling [2] and for the energy spread [8].

of the energy loss and the particle energy spread. However, in the region up to the maximum of the Bragg curve ( $R < R_0$ ) the experimental values of  $B(R)$  turned out to be much larger than the calculated ones. This discrepancy can be attributed, at least in part, to multiple Coulomb scattering of the particles that are stopped in the substance, allowance for which leads to an increase in the calculated values of  $B(R)$  when  $R \lesssim R_0$ , and to a decrease of the apparent range of the particles<sup>[3,6,7]</sup>. Earlier investigations of the Bragg curve were limited to a narrow region of ranges near  $R_0$ , and the influence of the nuclear interaction of the stopped particles with the substance on the form of the Bragg curve was not taken into account (owing to the knock-out of the particles as a result of the nuclear interaction, the values of  $B(R)$  at small values of  $R$  should increase considerably compared with  $B(R \approx R_0)$ ).

The purpose of the present investigation was to measure the Bragg curves for protons and other heavy particles with momentum  $\approx 1.3$  GeV/c in a wide interval of ranges  $R$ , and to compare them with the results of calculations by the Monte-Carlo method, in which account is taken of straggling, the energy spread of the particles, and scattering and nuclear knock-out of the particles. Since the scattering effect depends strongly on the geometry of the experiment, the measurements and calculations of the Bragg curves were performed for different relative placements of the ionization chamber and of the stopping substance.

## 2. MEASUREMENT OF THE BRAGG CURVES

The experiments were performed with beams of protons, deuterons, and  $\alpha$  particles extracted from the chamber of the synchrocyclotron of the Nuclear Problems Laboratory of JINR. The  $B(R)$  dependence was measured with the aid of an ionization chamber of 8 cm diameter, the current of which was registered with an automatic recording potentiometer. The thickness of the stopping filter  $R$ , which had the shape of a wedge, was varied in synchronism with the motion of the potentiometer chart. This has made it possible to record the Bragg curve continuously. To monitor the intensity of the beam we used an ionization chamber located in front of the stopping filter. The diameter of the beam entering the stopping filter was 2 cm, and the transverse dimensions of the filter were 20 cm.

The Bragg curves  $B(R)$  measured for copper and lead are shown in Figs. 2–4. The same figure shows the  $B_0(R)$  plots calculated with allowance only for the straggling and for the energy spread of the beam<sup>1)</sup>. In

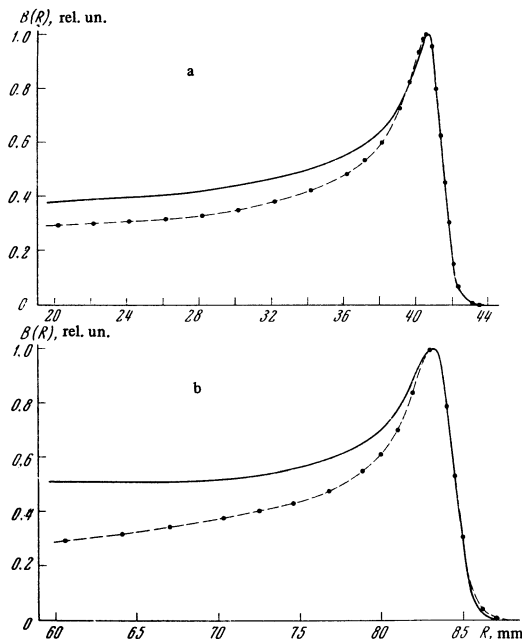


FIG. 2. Bragg curve for  $\alpha$  particles (a) and for deuterons (b) in copper; solid curve— $B(R)$  dependence, points and dashed curve—calculated values of  $B_0(R)$ .

the calculation of the  $B_0(R)$ , the spread  $\Delta R$  of the particle ranges was approximated by a Gaussian function  $G(R, \Delta R)$ , the dispersion of which was determined on the basis of the calculations of Sternheimer<sup>[2]</sup> and the measurement result of<sup>[8]</sup>. The  $B(R)$  and  $B_0(R)$  plots were normalized to unity at the maximum  $B(R)_{\max}$  and were made to coincide on the  $R$  scale at the point  $R_{0.8}$  corresponding to  $B(R_{0.8}) = 0.8 B(R)_{\max}$ , which is not very sensitive to changes of the parameters of the calculated  $B_0(R)$  curve<sup>[4]</sup>.

As seen from Fig. 2a, in the case of  $\alpha$  particles, for which the effects of scattering and nuclear knock

<sup>1)</sup>The values of  $B_0(R)$  calculated by us in the region  $R < R_0$  slightly exceed the values obtained by Mather and Segre<sup>[4]</sup>, who used an approximate  $dE/dR$  dependence in their calculations.

out should be relatively small, the measured  $B(R)$  plots and the calculated  $B_0(R)$  curves are close to each other. For protons, which have a smaller mass and a larger range, the effects of interaction with the stopping substance play a much larger role. Correspondingly, there is an appreciable difference (Figs. 3 and 4) between the experimentally obtained Bragg curves and the calculated  $B_0(R)$ . This difference is particularly large in the region of small  $R$ . Deuterons (Fig. 2b) occupy an intermediate position between  $\alpha$  particles and protons.

## 3. CALCULATION OF BRAGG CURVES. DISCUSSION

As seen from Fig. 3, the form of the experimentally obtained Bragg curves changes considerably when the distance  $l$  between the ionization chamber and the stopping filter changes. This shows that scattering of the particles in the stopping substance has a strong influence on the form of the Bragg curve, and that the calculation of the  $B(R)$  curves used for the description of the experimental data must be carried out under the same geometrical conditions as in the measurement of the Bragg curves. The calculation of the  $B(R)$  curves was carried out in several successive stages. In the first stage, we took into account only multiple Coulomb scattering of the stopped protons. The stopping filter of thickness  $R$  was subdivided into a large number of

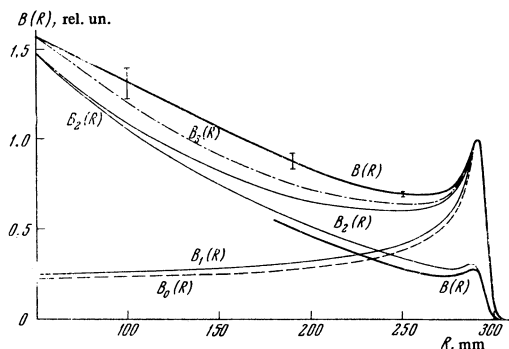


FIG. 3. Measured Bragg curves  $B(R)$  (heavy lines) for protons in copper at  $l = 8$  cm (upper curve) and  $l = 30$  cm (lower curve), and the calculated curves, which take into account successively the beam proton energy spread and the straggling ( $B_0$ ), multiple Coulomb scattering ( $B_1$ ), nuclear interaction ( $B_2$ ), and meson production ( $B_3$ ). The curves are normalized at  $l = 8$  cm (see the text).

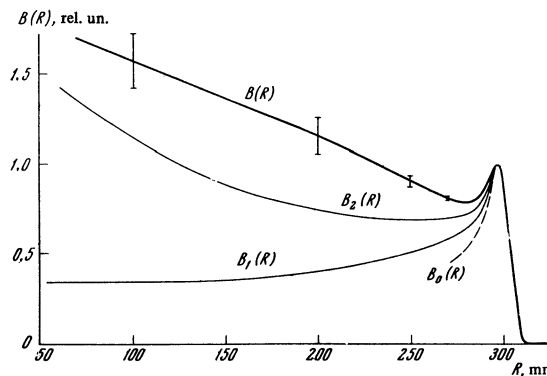


FIG. 4. The same as in Fig. 3, but for lead ( $l = 8$  cm). The  $B_3(R)$  dependence differs little from  $B_2(R)$ , since the correction for meson production is small in the case of lead.

layers, and the scattering of the protons in each layer was determined by the Monte Carlo method. The thickness  $R$  was increased in succession, and the trajectory of each particle was traced until it entered the ionization chambers (or else the protons were stopped in the substance or traveled past the chamber). Altogether from 5000 to 20,000 such events were tried for each of the chosen values of  $R$ . As a result of the calculation, we obtained the distribution of the particles with respect to  $R'$ ,  $F(R, R')$ , and with respect to the cosine of the scattering angle at 18 fixed values of  $R$ . Typical  $F(R, R')$  distributions are shown in Fig. 5.

Further, by integrating the obtained distributions and the ionization losses (2), we calculated the ionization-chamber current  $B'(R)$  and the convolution  $B_1(R)$  of this function with the curve representing the spread of the particle ranges  $G(R, \Delta R)$  (see above). The  $B_1(R)$  plots obtained in this manner describe the Bragg curves without allowance for the nuclear interaction between the protons and the stopping substance. These plots are shown in Figs. 3 and 4.

From Fig. 3, which shows the Bragg curves for copper, we see that the calculated values of  $B_1(R)$  are in good agreement with the experimental data in the region beyond the maximum of the Bragg curve. The average energy spread of the beam protons, determined from this part of the Bragg curve, is  $2.7 \pm 0.3$  MeV, which coincides with the experimentally obtained value  $2.8 \pm 0.3$  MeV<sup>[8]</sup>. In the region up to the maximum of the Bragg curve, the calculated  $B_1(R)$  curves for copper lie much lower than the experimental  $B(R)$  plot. A similar difference is obtained also for lead (Fig. 4). From a comparison of the  $B_0(R)$ ,  $B_1(R)$ , and  $B(R)$  curves we see that allowance for the multiple Coulomb scattering of the particles decreases only little the discrepancy between the measured and calculated Bragg curves, which is particularly large in the region of small  $R$ .

This discrepancy can be eliminated to a considerable degree if account is taken, in the calculation of  $B(R)$ , of the knock-out of the protons due to the nuclear interaction during the course of their stopping in the substance. Simple estimates show that in a range of  $\approx 30$  cm of copper approximately 90% of the protons experienced nuclear interactions that resulted in the

disintegration of the nuclei of the substance, in elastic scattering of the protons, or in meson production. The correction to the  $B_1(R)$  needed to account for the nuclear interaction of the protons, was calculated in accordance with the following simplified scheme: it was assumed that the inelastic interactions and half of the elastic interactions of the protons with the nuclei of the substance lead to knock out of protons. For the inelastic and elastic scattering cross sections we used the experimental data systematized by W. Lock (private communication). The  $B_2(R)$  plot obtained as a result of this correction for copper is shown in Fig. 3. This plot is in good agreement with the experimental values in the region beyond the maximum of the Bragg curve. The average energy spread of the beam protons obtained from a comparison of the  $B(R)$  and  $B_2(R)$  curves is  $2.9 \pm 0.3$  MeV, and agrees with the direct measurements<sup>[8]</sup>. At smaller values of  $R$ , the  $B_2(R)$  curves are close to the measured Bragg curves. Allowance for the meson production processes (the  $B_3(R)$  curve) brings the calculated and measured Bragg curves even closer together. In the case of lead, the discrepancy between the calculated and measured Bragg curves remains appreciable also after corrections are introduced for the nuclear interaction of the protons (Fig. 4); this apparently is a reflection of the approximate character of the calculation, in which no account is taken, for example, of the fact that the ionization chamber registers also the nuclear disintegration products.

The measurement and calculation of the Bragg curves were performed also for substances with a smaller nuclear charge (aluminum, carbon, polyethylene  $CH_2$ ). Here, too, a large discrepancy is observed between the  $B(R)$  and  $B_0(L)$  curves in the region of small  $R$ . Multiple Coulomb scattering of the protons in these substances is much smaller than in copper and lead, and allowance for this scattering changes little the form of the calculated Bragg curve. When corrections are introduced for the nuclear interaction of the stopped protons, the agreement between the measured and calculated Bragg curves turned out to be the same as in Fig. 3.

In order to verify the assumed calculation scheme, we measured and calculated the Bragg curves for a smaller ionization chamber (2 cm diameter) located at different distances  $y$  from the beam axis. Figure 6 shows plots of two characteristics of the Bragg curve—the maximum of the Bragg curve  $B(R)_{\max}$  and the

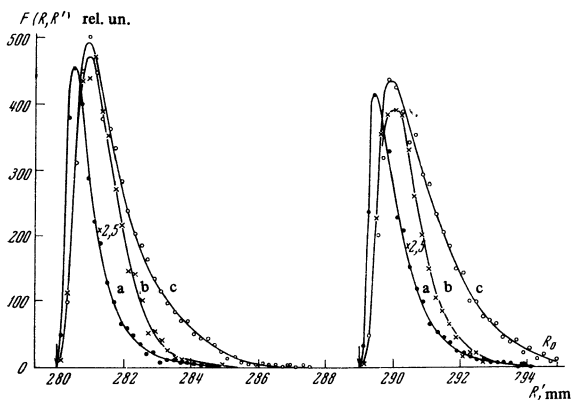


FIG. 5. Distributions  $F(R, R')$  for protons in copper (a) and in lead (b, c) at  $l = 4$  cm (a, c) and  $l = 12$  cm (b). The values of  $R$  are indicated by the arrows,  $R_0 = 295$  mm.

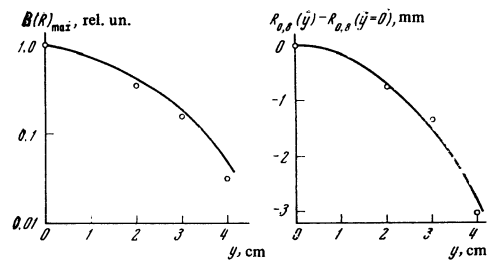


FIG. 6. Dependence of the maximum of the Bragg curve  $B(R)_{\max}$  and of the position of the point  $R_{0,8}$  corresponding to  $B(R_{0,8}) = 0.8 B(R)_{\max}$  on the displacement of the chamber  $y$  relative to the beam axis. Curve—calculation result, point—experimental data.

point  $R_{0.8}$  (see above)—as functions of  $y$ . As seen from Fig. 6, the calculated values agree with the measurement results.

The foregoing comparison of the measured and calculated Bragg curves shows that at proton energies  $\gtrsim 600$  MeV the form of the Bragg curve is determined to a considerable degree by the nuclear interaction of the protons stopped in the substance. This effect must be taken into account in determining particle energies by the Bragg-curve method.

In conclusion, we take the opportunity to thank W. Lock for kindly supplying the data of his review prior to their publication.

<sup>1</sup>M. S. Walske, Phys. Rev. 88, 1283 (1952); 101, 940 (1956).

<sup>2</sup>R. M. Sternheimer, Phys. Rev. 88, 851 (1952); 91, 256 (1953); 103, 511 (1956).

<sup>3</sup>I. M. Vasilevskiĭ and Yu. D. Prokoshkin, JINR Preprint D-566, 1960; Yad. Fiz. 4, 549 (1966) [Sov. J. Nucl. Phys. 4, 390 (1967)].

<sup>4</sup>R. Mather and E. Segre, Phys. Rev. 84, 191 (1951).

<sup>5</sup>V. P. Zrellov and G. D. Stoletov, Zh. Eksp. Teor. Fiz. 36, 658 (1959) [Sov. Phys.-JETP 9, 461 (1959)].

<sup>6</sup>C. N. Yang, Phys. Rev. 84, 599 (1951).

<sup>7</sup>H. Bichel, Phys. Rev. 120, 1012 (1960); Univ. of South Calif. Tech. Rep. 2, 3 (1961).

<sup>8</sup>I. M. Vasilevskiĭ and Yu. D. Prokoshkin, Atomnaya énergiya 7, 225 (1959).